Hindawi
Advances in Civil Engineering
Volume 2020, Article ID 8888550, 13 pages
https://doi.org/10.1155/2020/8888550

Research Article

Effect of Particle Size on the Hydraulic Characteristics of Mechanically and Biologically Treated Waste

Zhenying Zhang, Xiufeng Pan, Jiahe Zhang, and Hui Xu

School of Civil Engineering and Architecture, Zhejiang Sci-Tech University, Hangzhou 310018, China

Correspondence should be addressed to Zhenying Zhang; zhangzhenyinga@163.com

Received 9 May 2020; Revised 2 September 2020; Accepted 10 September 2020; Published 19 September 2020

Academic Editor: Chunshun Zhang

Mechanical biological treatment (MBT) is a waste processing technology that helps conserve resources and reduce emissions harmful to the environment. The treatment of municipal solid waste (MSW) using MBT is a hot topic in environmental geotechnical engineering. Permeability tests were carried out on MBT waste using a compression and permeability combined apparatus and a large-scale vertical permeability apparatus taking the influence of particle size into consideration. The permeability of samples with smaller particle sizes was found to be lower for the same pressure and dry mass (%) of component. The best-fit line between the logarithmic permeability and variables such as the dry density was linear. As the dry density increased or the void ratio decreased, the permeability of samples with smaller particles decreased more. The logarithmic permeability increased with the increase in the average particle size and void ratio. The permeabilities of MBT waste corresponding to particle size ranges of 0–10, 0–20, and 0–40 mm were 10^{-10}–10^{-5}, 10^{-8}–10^{-4}, and 10^{-5}–10^{-3} m/s, respectively. The difference between MBT waste and MSW was analyzed in terms of their permeability. The results of MBT waste were compared with those reported in previous studies to provide reference for the permeability analysis of MBT landfills.

1. Introduction

Mechanical biological treatment (MBT) has attracted increased research interest since it was proposed in the late 1990s [1, 2]. The MBT technology involves screening and shredding by mechanical treatment, selecting large-sized plastic by hand and recyclable materials by magnetic separation, and finally treating the organic materials by biological treatment; the remaining waste is disposed to landfills [3, 4]. Converting waste to a biostable and low-moisture MBT waste can help decrease the volume, leachates, and gas content in landfills, thus reducing the harmful effects of methane on the environment [5, 6].

MBT waste has varied characteristics because it contains municipal solid waste (MSW) from different regions. Adani et al. [7] found that in Italy the input raw materials (MSW) are treated differently in the MBT process. The waste (<50 mm) is biologically treated and later landfilled after decreasing the particle size to less than 20 mm through mechanical sieving and biological recycling. Zhang et al. [8] obtained different grain size distribution of MBT waste (from UK) with different shredding treatment. Kuehle-Weidemeier [9] found the uniformity coefficients of MBT waste (from Germany) with particle size ranges of 0–60, 0–40, and 0–20 mm to be 50, 123, and 192, respectively. In another study, Tungtakanpoung [10] determined different contents of the components of MBT waste (from Thailand) with three particle size ranges (<10, 10–40, and >40 mm); the results were quite different from the results of MBT waste in Italy [11].

The particle size significantly influences the permeability of MBT waste. Ziehmann et al. [12] found that the permeabilities of MBT waste with particle size ranges of 0–60, 0–40, and 0–30 mm are in the ranges of 4.35×10^{-8}–1.63×10^{-5}, 2.6×10^{-8}–1.04×10^{-5}, and 3.76×10^{-8}–6.61×10^{-6} m/s, respectively. Siddiqui [13] found the ranges of the permeability of MBT waste with particle size ranges of 0–60 and 0–20 mm to be 5.3×10^{-7}–6.6×10^{-5} and 8×10^{-7}–7.8×10^{-5} m/s, respectively. Table 1 lists the permeabilities of MBT waste with different particle sizes.

Table 1: Permeability of MBT waste with different particle sizes.

Authors	Particle size (mm)	σ (kPa)	ρ_d (g/cm^3)	D (mm)	Biological treatment	Test method	k (m/s)
Ziehmann et al. [14]	0–16	—	—	—	Aerobic	Surface	3×10^{-8}–3×10^{-7}
	0–40					Runoff	3×10^{-7}–3×10^{-6}
Heiss-Ziegler and Fehrer [15]	0–25	—	—	—	Aerobic	–	6.2×10^{-11}–1.8×10^{-10}
	0–40						2.4×10^{-10}–1.1×10^{-7}
Ziehmann et al. [12]	0–30	—	—	—	Anaerobic	–	3.76×10^{-8}–6.61×10^{-6}
	0–40				Aerobic		2.60×10^{-8}–1.04×10^{-5}
	0–60						4.35×10^{-8}–1.63×10^{-5}
Felske et al. [16]	0–40	—	—	—	Aerobic	–	9.0×10^{-6}–3.2×10^{-5}
Kuehle-Weidemeier [9]	0–20	—	0.77	180	Aerobic tunnel	–	7.8×10^{-8}
			0.8	180			3.7×10^{-9}
			0.81	600			2.3×10^{-10}
	0–40	—	0.71	180			3.6×10^{-6}
			0.7	180			6.5×10^{-6}
			0.85	600			7.0×10^{-10}
	0–60	—	0.75	180			6.2×10^{-6}
			0.6	180			5.2×10^{-5}
			0.86	600			1.8×10^{-8}
	0–30	50–550	0.69–0.92	600	Composted		5.6×10^{-9}–3.1×10^{-6}
Xie et al. [17]	0–6.3	—	1.10	100	Degraded M1	Triaxial	8.5×10^{-8}
	0–20		1.11		Sample		6.3×10^{-10}
	0–40		0.85		Degraded M2		1.6×10^{-9}
	0–60		0.80		Sample		1.8×10^{-7}
	0–40		0.85		Degraded M3		7.8×10^{-9}
	0–60		0.80		Sample		2.0×10^{-7}
Petrović et al. [18]	0–40	36–365	—	800	Aerobic	—	2.3×10^{-9}–7.4×10^{-8}
Zardava et al. [22]	0–10	—	0.52	260	—	Constant head	1×10^{-5}–5×10^{-5}
Izzo et al. [20]	0–4	—	0.49–0.82	101.5	—	—	1.8×10^{-8}–4×10^{-6}
Woodman et al. [19]	0–20	50	–	480	—	—	5.9×10^{-6}–6.6×10^{-6}
		150					6.7×10^{-7}–8×10^{-7}
Siddiqui [13]	0–20	0–150	0.44–0.71	480	Composted	Constant head	8×10^{-7}–7.8×10^{-5}
	0–60				Anaerobic		5.3×10^{-7}–6.6×10^{-5}
Pimolthai and Wagner [21]	0–10	—	0.7	100	Aeration rotting tunnels	Falling head	7.7×10^{-7}
			1.0		Composting		1.9×10^{-8}
			0.9		Composting		6×10^{-9}

Note. σ (kPa) pressure; ρ_d (g/cm^3) dry density; D (mm) specimen diameter; k (m/s) permeability.

The relationship between the permeability and the pressure of MBT waste (Table 1) with one particle size has been studied by several researchers [9, 18, 19]. In addition, the relationship between the permeability and the dry density of MBT waste with one particle size has also been studied [20, 21]. In this study, a systematic analysis on the MBT waste (from Hangzhou, China) with different particle size ranges (0–10, 0–20, and 0–40 mm) was carried out using a compression and permeability combined apparatus and a large-scale vertical permeability apparatus. The relationships between the permeability and the variables such as the dry density were established taking the impact of particle size into consideration. The hydraulic characteristics were analyzed by comparing the wastes in relevant countries.

2. Materials and Methods

2.1. Materials. Figure 1 shows the MBT process of MSW adopted from a pilot MBT project at the Tianziling Landfill (in Hangzhou, China) in the subtropical monsoon climate zone, which is warm and humid [23]. Plastic, textiles, and metal were recovered by mechanical treatment, the remaining waste was hydrolyzed, and the MBT waste was kept in the workshop for drying treatment.

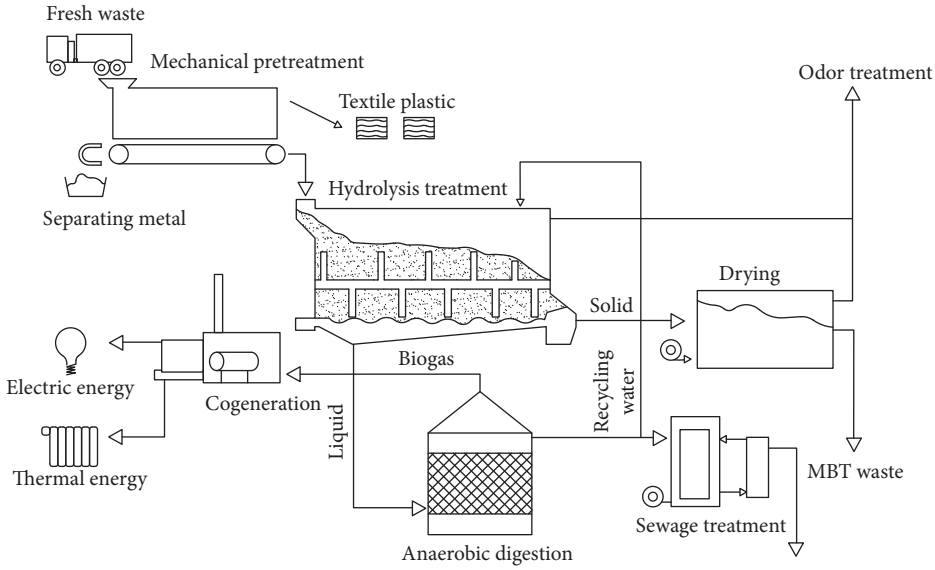

Figure 1: Schematic of mechanical biological treatment (MBT) of municipal solid waste (MSW).

The materials with the quantities of almost 70 barrels were obtained from several workshops and transported to the environmental geotechnical laboratory. The capacity of each barrel was 120 L. Samples of the materials used for the tests were selected using the quartile method. Three round sieves with sizes of 10, 20, and 40 mm were, respectively, placed on three top dual-purpose screen shakers and the original MBT waste was placed in the sieves. A portion of the materials was passed through the sieves after shaking for 15–20 min and the samples of P1-1 (0–10 mm), P1-2 (0–20 mm), and P1-3 (0–40 mm) were, respectively, obtained from the materials under the sieves. After preparing samples P1-1, P1-2, and P1-3, three round sieves with sizes of 10, 20, and 40 mm were also placed on three top dual-purpose screen shakers, respectively. The original waste was also placed in the sieves, then crushed, and shaken until all the materials in the sieve passed through their respective round sieves. Samples of P2-1 (0–10 mm), P2-2 (0–20 mm), and P2-3 (0–40 mm) were, respectively, obtained from the materials under the sieves. The type of components in the samples (P1-1, P1-2, and P1-3) is the same as that in the original MBT waste; however, the dry mass (%) of the components is different. The types and dry mass (%) of components in the samples P2-1, P2-2, and P2-3 and the original MBT waste are the same. Therefore, the dry mass (%) of components in the samples P1-1, P1-2, and P1-3 and that in the samples P2-1, P2-2, and P2-3 are different.

Figure 2 shows the type and dry mass (%) of components in samples P1-1 (0–10 mm), P1-2 (0–20 mm), and P1-3 (0–40 mm) and the original MBT waste (same as samples P2-1, P2-2, and P2-3) obtained from the component analysis. The unidentified component is the one that could not be identified or crushed, whereas fine components are those that are finer than 5 mm. The P1-1 sample contained fines (48.4%) and wood (25.8%). The P1-2 sample contained fines (28.5%), rubber and plastic (20.8%), wood (18.7%), textiles (12.4%), and glass (12.3%). The P1-3 sample contained rubber and plastic (24%), wood (14.8%), textile (14.7%), and glass (14.7%). The original MBT waste contained rubber and plastic (30.9%), textile (16.8%), fines (16%), wood (11.5%), and glass (11.3%). P1-1 had the highest fine component content, whereas the original MBT waste had the least. However, the rubber and plastic component content in P1-1 was the least, whereas the original MBT waste had the highest. The metal components in the P1-1, P1-2, P1-3, and the original MBT waste were less. Plastics and textiles accounted for a larger proportion of the MBT waste samples with larger particle sizes; fines accounted for a larger proportion with smaller particle sizes. Thus, plastics and textiles were mainly of a large size, and the fines were mainly fine particles. A correlation exists between the dry mass (%) of the component and the particle size.

2.2. Testing Apparatus. Compression and permeability related tests were conducted to determine the permeability of MBT waste with smaller particle sizes (0–10 and 0–20 mm) using a compression and permeability combined apparatus considering the effects of pressure (Figure 3(a)) [24]. A maximum vertical pressure of 1600 kPa could be applied to the permeation column using a lever. The diameter and height of the permeation column were 150 and 347 mm, respectively. A cylindrical header tank was fixed on an adjustable plate with a maximum height of 1200 mm. The hydraulic gradient was set by varying the height of the header tank. Large-scale vertical permeability tests were conducted to determine the permeability of MBT waste with larger particle sizes (0–40 mm) using a large-scale vertical permeability apparatus (Figure 3(b)) [25]. The diameter and height of the permeation column were 400 and 800 mm, respectively. The hydraulic gradient was set by varying the height of the header tank.

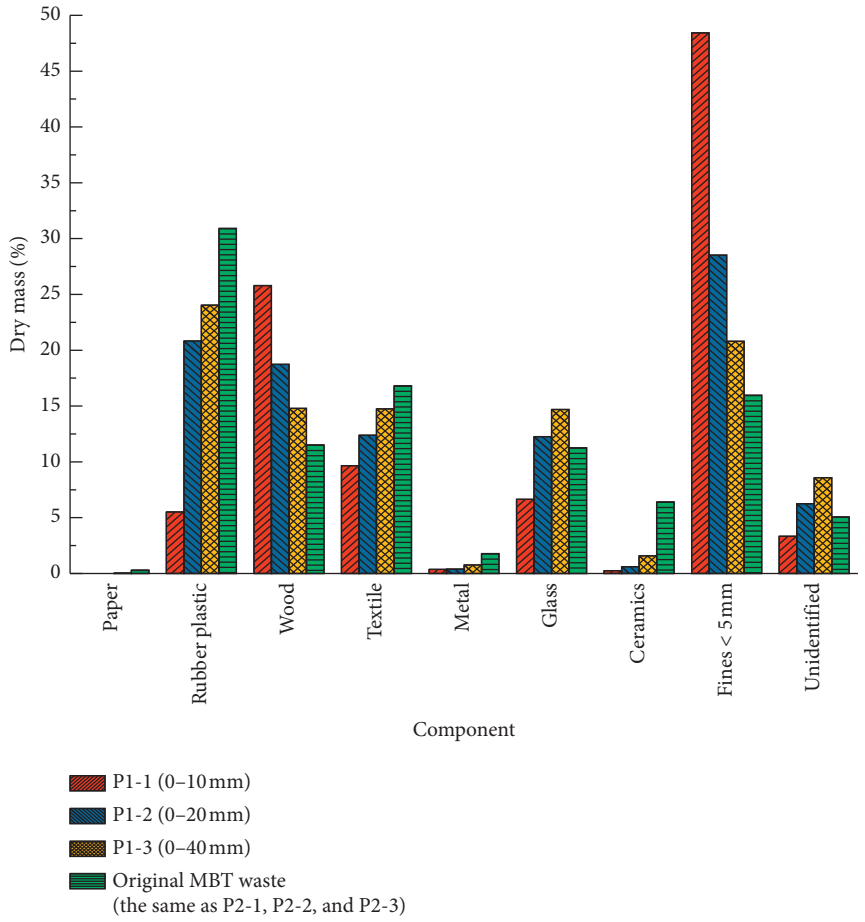

Figure 2: Various components in MBT waste samples with different particle sizes.

2.3. Experimental Procedure. The grain size analysis tests and permeability tests were conducted in accordance with the Chinese Technical Specification for Soil Test of Landfilled Municipal Solid Waste (CJJ/T204-2013) [26]. Permeability tests were conducted on the samples P1-1, P2-1, P1-2, and P2-2 using a compression and permeability combined apparatus taking the effect of pressure into consideration. Permeability tests were conducted on the samples P1-3 and P2-3 using a large-scale vertical permeability apparatus to avoid the scale effect. For this study, 540 groups of permeability tests were conducted and the materials with the quantities of almost 5 barrels were processed.

2.3.1. Grain Size Analysis Tests. Dried samples of P1-1 (0–10 mm) and P2-1 (0–10 mm) were shaken for 15–20 min using sieves with sizes of 5, 2, 1, 0.5, 0.2, 0.1, and 0.075 mm. The mass of each sieve was determined, and the ratio of the mass lower than a certain particle size to the total mass was calculated. The grain size distribution curves of P1-1 and P2-1 were obtained. Dried samples of P1-2 (0–20 mm) and P2-2 (0–20 mm) were shaken for 15–20 min using sieves with sizes of 10, 5, 2, 1, 0.5, 0.2, 0.1, and 0.075 mm; the aforementioned calculations were carried out, and the grain size distribution curves were obtained. Dried samples of P1-3 (0–40 mm) and P2-3 (0–40 mm) were shaken for 15–20 min using sieves with sizes of 20, 10, 5, 2, 1, 0.5, and 0.2 mm; the aforementioned calculations were carried out, and the grain size distribution curves were obtained. A dried sample of the original MBT waste was shaken for 15–20 min using sieves with sizes of 60, 40, 20, 10, 5, 2, and 1 mm. The same calculation method was employed, and the grain size distribution curve of the original MBT waste was obtained.

2.3.2. Compression and Permeability Related Tests. Permeability tests were conducted on the samples P1-1, P2-1, P1-2, and P2-2 at pressures of 50, 100, 200, 300, and 400 kPa, each with six hydraulic gradients. The permeation rate was small under the small hydraulic gradient. Hydraulic gradients of 2, 1.75, 1.5, 1.25, 1, and 0.5 were set under pressures of 50 and 100 kPa, and gradients of 5, 4.5, 4, 3.5, 3, and 2.5 were set under pressures of 200, 300, and 400 kPa. 360 groups of permeability tests were conducted and the samples with the quantities of almost 2 barrels were processed.

Consider sample of P1-1 under a pressure of 50 kPa with hydraulic gradients of 2, 1.75, 1.5, 1.25, 1, and 0.5 as an example to explain the method of the test. The sample was selected using the quartile method and placed in a constant temperature oven at 65°C for drying. The dried sample was placed into the permeability column five times and

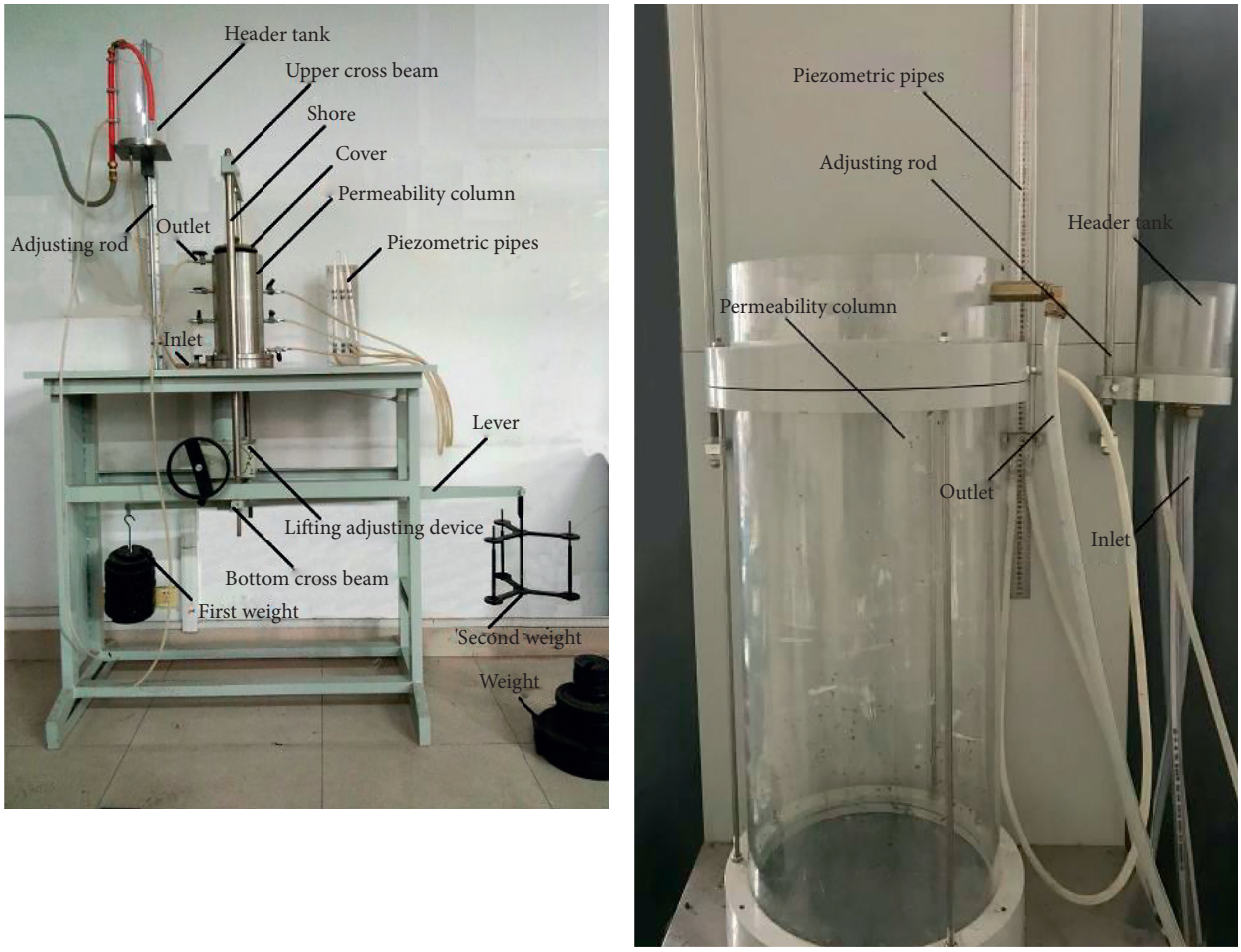

(a) (b)

Figure 3: Permeability apparatus. (a) Compression and permeability combined apparatus. (b) Large-scale vertical permeability apparatus.

compacted to ensure a uniform sample. Filter paper and porous stone were placed at both ends of the sample. The total mass (M_1) and initial height (H_1) of the sample were recorded. The permeability column was fixed after pushing it under the cover. Water flowed from the head tank to the inlet. After achieving a stable outflow, the sample was saturated. Then, a pressure of 50 kPa was set and the hand wheel was adjusted to keep the lever level. The permeability test was conducted after compressing the sample for 24 h. The settlement (S) was recorded, and the height of the sample compressed for 24 h was calculated using equation $H' = H_1 - S$. The hydraulic gradient was set as 2, and the height of the header tank was adjusted. Three parallel tests were performed after the flow of water became stable. The hydraulic gradients were reduced to 1.75, 1.5, 1.25, 1, and 0.5. After the test with six hydraulic gradients was completed, the weight was removed, and the sample was taken out.

The above steps were repeated to refill the sample of P1-1, and the following tests were conducted under pressures of 100, 200, 300, and 400 kPa, respectively. The data were recorded until all the tests have been completed.

2.3.3. Large-Scale Vertical Permeability Tests. Permeability tests were conducted on the samples P1-3 and P2-3 with hydraulic gradients of 1.25, 1, 0.75, 0.5, 0.25, and 0.1.

Consider sample P1-3 as an example to explain the method of the test. The sample was selected using the quartile method and placed in a constant temperature oven at 65°C for drying. The dried sample was placed into the permeability column five times and compacted to ensure a uniform sample. Filter paper and porous stone were placed at both ends of the sample. The total mass (M_2) and initial height (H_2) of the sample were recorded. The water flowed from the head tank to the inlet. After achieving a stable outflow, the sample was saturated. An initial hydraulic gradient of 1.25 was set, and the height of the header tank was adjusted. Three parallel tests were conducted after the flow of water became stable. The hydraulic gradients were reduced to 1, 0.75, 0.5, 0.25, and 0.1. After the test with six hydraulic gradients has been completed, the sample was taken out.

The above steps were repeated to refill the sample of P1-3, and the dry density was varied by increasing the

compaction and stacking weight. Tests were conducted on P1-3 with dry densities of 0.150, 0.154, 0.166, 0.205, and 0.223 g/cm^3, whereas tests were conducted on P2-3 with dry densities of 0.299, 0.339, 0.357, 0.400, and 0.417 g/cm^3. 180 groups of permeability tests were conducted and the samples with the quantities of almost 3 barrels were processed. The data were recorded until all the tests were completed.

3. Results

3.1. Grain Size Analysis. Figure 4 shows the grain size distribution curves under different particle sizes. The percentages of P1-1, P2-1, P1-2, P2-2, P1-3, P2-3, and the original MBT waste that passed through a 5 mm sieve were 36.0, 26.9, 26.8, 25.2, 24.7, 19.5, and 16.0, which decreased in this order. Table 2 lists the characteristic particle sizes (d_{10}, d_{30}, d_{50}, and d_{60}, which are diameters of the particle size at which 10%, 30%, 50%, and 60% of the materials pass through the sieve), uniformity coefficient (C_u), and curvature coefficient (C_c) of P1-1, P1-2, P1-3, P2-1, P2-2, P2-3, and the original MBT waste. The uniformity coefficients of P1-1, P1-2, P1-3, P2-2, P2-3, and the original MBT waste are greater than 5, and the curvature coefficient is in the range of 1–3. Samples of P1-1, P1-2, P1-3, P2-2, P2-3, and the original MBT waste are well-graded waste, whereas P2-1 is not.

3.2. Hydraulic Characteristics

3.2.1. Relationship between Permeability and Pressure. Figure 5 shows the relationship between the permeability and pressure of P1-1, P2-1, P1-2, and P2-2. The best-fit line between the logarithmic permeability (lg$k$) and the pressure (σ) is linear (equation (1)). Table 3 lists the coefficients A and B and the correlation coefficient R^2.

$$\lg k = A + B\sigma. \quad (1)$$

As shown in Figure 5, the permeabilities of P2-1 and P2-2 are in the range of 10^{-4}–10^{-3} m/s, whereas the permeabilities of P1-1 and P1-2 are in the range of 10^{-5}–10^{-4} m/s under a pressure of 0 kPa. Furthermore, the permeabilities of P2-1 and P2-2 are in the range of 10^{-10}–10^{-7} m/s, whereas the permeabilities of P1-1 and P1-2 are in the range of 10^{-8}–10^{-6} m/s under a pressure of 400 kPa. Therefore, the permeabilities of P2-1 and P2-2 decreased to a greater extent with increasing pressure, and the slope of the best-fit line of P2-1 and P2-2 is greater than that of P1-1 and P1-2. The permeability of P2-1 became lower than that of P1-1 when the pressure increased slightly above 150 kPa. The permeability of P2-2 became lower than that of P1-2 at pressures that are slightly below 150 kPa. As a result of the heterogeneity and high compressibility of the MBT waste, the main components had an effect on permeability. Scanning electron microscope (SEM) images (see Figure 6) of the components of plastic and textile in the MBT waste were obtained at a magnification of 500. As the plastic surface has no pores, the large-sized plastic changed the vertical seepage path and reduced the vertical permeability under compaction conditions [16]. The textile was largely filled with impurities, and the pores inside the fiber were significantly reduced. The main reason could be that the samples P2-1 and P2-2 contained more rubber, plastics, and textiles, but less fines. The compression of rubber plastics and textiles is less at pressures below 150 kPa, and the interparticle voids between the components are relatively large. The degree of compression of samples P2-1 and P2-2 is increased with the increase in the pressure. The components were further compressed under a pressure of more than 150 kPa, and the interparticle voids were relatively reduced.

As the best-fit line of P2-1 (0–10 mm) was located below that of P2-2 (0–20 mm), the permeability of P2-1 was lower than that of P2-2 under the same pressure. When the component and content of the sample were the same, the permeability of the smaller particle sizes was lower, which is consistent with results in previous studies [9, 14, 15]. As the best-fit line of P1-1 (0–10 mm) was located below that of P1-2 (0–20 mm), the permeability of P1-1 was lower than that of P1-2 under the same pressure. The permeabilities of P2-1 and P2-2 were slightly lower than those of P1-1 and P1-2 under a pressure of 400 kPa. There were differences in the particle size and component content in the samples, indicating that the influence of particle size on the permeability is less than that of the component content under a pressure of 400 kPa.

3.2.2. Relationship between Permeability and Dry Density. Figure 7 shows the relationship between the permeability and the dry density of samples with different particle sizes. The best-fit line between the logarithmic permeability (lg$k$) and the dry density (ρ_d) is linear (equation (2)). Table 4 lists the coefficients C and D and the correlation coefficient R^2.

$$\lg k = C + D\rho_d. \quad (2)$$

Figure 7 shows that the absolute values of the slopes of the best-fit lines (P1-1, P1-2, and P1-3) decrease sequentially with the increase in the particle size of the samples; similar results were obtained for P2-1, P2-2, and P2-3. The permeability of the samples with smaller particle sizes decreased to a greater extent with the increase in the dry density.

The absolute values of the slopes of the best-fit lines between P1-1 and P2-1 were essentially similar. The absolute value of the slope of the best-fit line of P1-2 was less than that of P2-2. The absolute value of the slope of the best-fit line of P1-3 was much lower than that of P2-3. The differences between the slopes of the samples (P1-1 and P2-1, P1-2 and P2-2, and P1-3 and P2-3) increased at increasing particle size. This may be due to the different contents in the samples, given that the particle size and component were the same. The difference in the interparticle voids increased with an increase in the particle size.

The permeability ranged from 4.9×10^{-3} to 5.24×10^{-10} m/s at a dry density range of 0.15–0.84 g/cm^3. As the dry density of samples P1-1, P1-2, and P1-3 was 0.7 g/cm^3, the permeability intervals of P1-2 (10^{-7}-10^{-6} m/s) and P1-3 (10^{-5}–10^{-4} m/s) were lower than that of P1-1 (10^{-4}-10^{-3} m/s). Xie et al. [17] obtained a similar result; namely, the permeability of the MBT waste with a particle

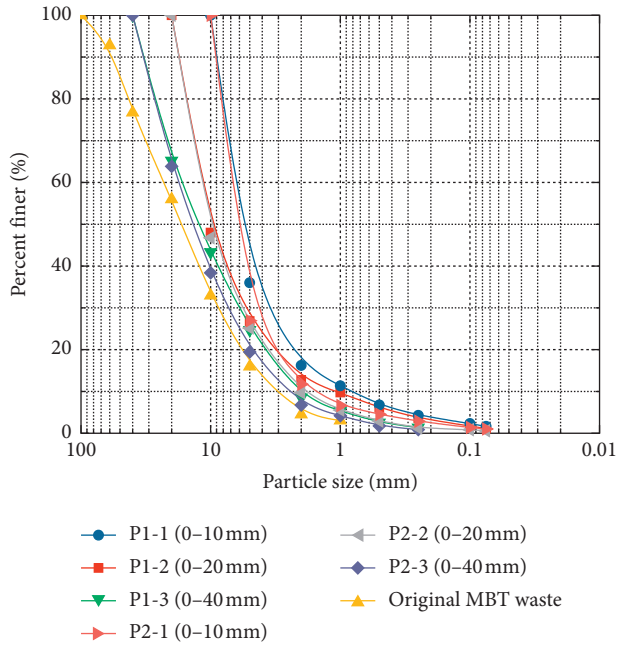

Figure 4: Grain size distribution curves of samples with different particle sizes.

Table 2: Results of particle size, uniformity coefficient, and curvature coefficient of MBT waste.

Sample	d_{10} (mm)	d_{30} (mm)	d_{50} (mm)	d_{60} (mm)	C_u	C_c
P1-1	0.8	3.5	5.4	6.4	8.0	2.4
P1-2	1.1	5.2	9.4	11.3	10.3	2.2
P1-3	2.0	6.0	12.4	16.4	8.2	1.1
P2-1	1.5	4.2	5.9	6.7	4.5	1.8
P2-2	1.8	5.7	9.6	11.4	6.3	1.6
P2-3	2.4	7.3	13.8	17.5	7.3	1.3
Original MBT waste	3.1	8.8	16.7	23.0	7.4	1.1

Note. d_{10}, d_{30}, d_{50}, and d_{60} denote diameters of the particle size at which 10, 30, 50, and 60% of the materials pass through the sieve, respectively; C_u, uniformity coefficient; C_c, curvature coefficient.

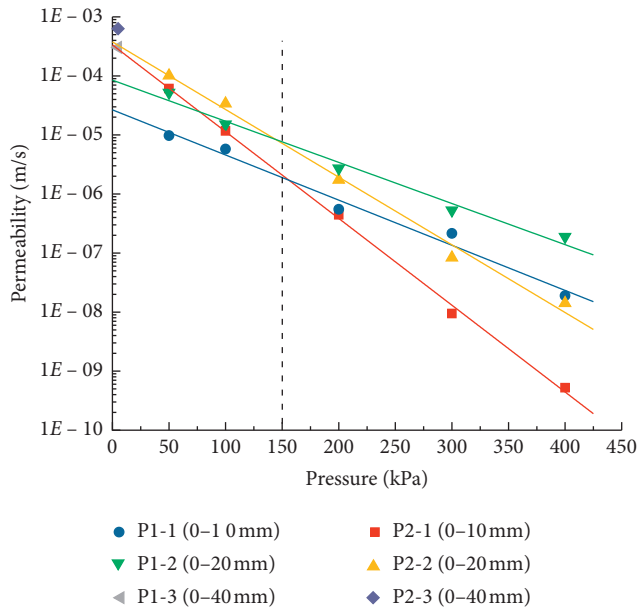

Figure 5: Relationship between the permeability and the pressure of samples with different particle sizes.

Table 3: Values of coefficients A and B and correlation coefficient R^2.

Samples	P1-1	P1-2	P2-1	P2-2
A	−4.57	−4.07	−3.47	−3.42
B (10^{-3})	−7.65	−6.96	−14.7	−11.46
R^2	0.982	0.984	0.998	0.992

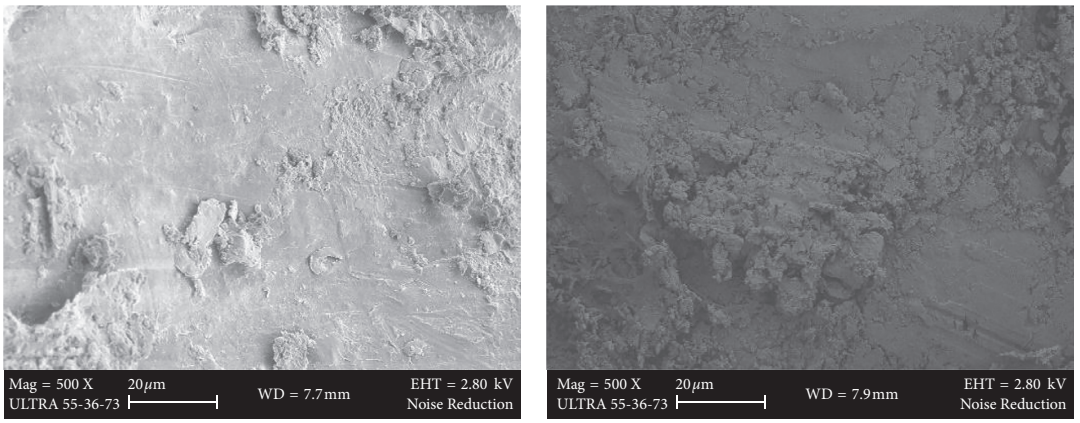

(a) (b)

Figure 6: SEM images of plastic and textile in MBT waste captured at a magnification of 500. (a) Plastic. (b) Textile.

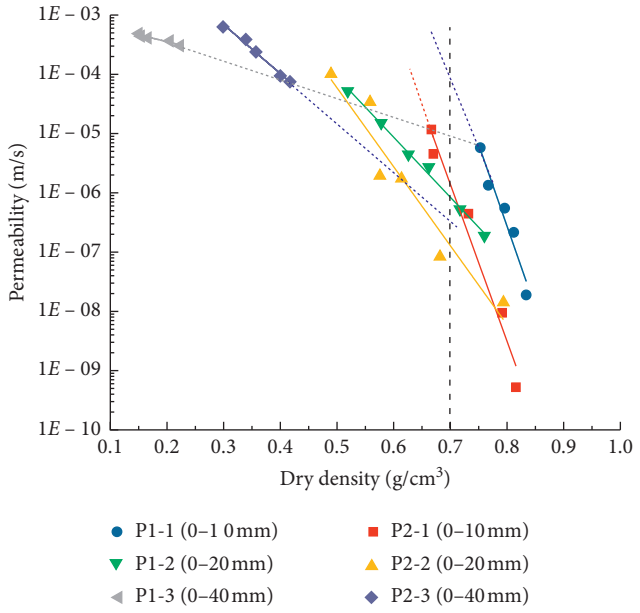

Figure 7: Relationship between the permeability and the dry density of samples with different particle sizes.

size range of 0–20 mm was lower than that of the MBT waste with a particle size range of 0–6.3 mm for the same dry density.

3.2.3. Relationship between Permeability and Void Ratio. Figure 8 shows the relationship between the permeability and the void ratio of samples with different particle sizes. The best-fit line between the logarithmic permeability (lg$k$) and the void ratio (lg$e$) is linear (equation (3)). Table 5 lists the coefficients E and F and the correlation coefficient R^2.

$$\lg k = E + F \lg e. \tag{3}$$

Figure 8 shows that the absolute values of the slopes of the best-fit lines of P1-1 (0–10 mm), P1-2 (0–20 mm), and P1-3 (0–40 mm) decrease in this order with the increase in the particle size, similar to the results obtained for P2-1 (0–10 mm), P2-2 (0–20 mm), and P2-3 (0–40 mm). The

Table 4: Values of coefficients C and D and correlation coefficient R^2.

Samples	P1-1	P1-2	P1-3	P2-1	P2-2	P2-3
C	15.43	1.02	−2.98	12.67	2.43	−0.68
D	−27.49	−10.13	−2.33	−26.47	−13.32	−8.27
R^2	0.928	0.993	0.909	0.961	0.909	0.981

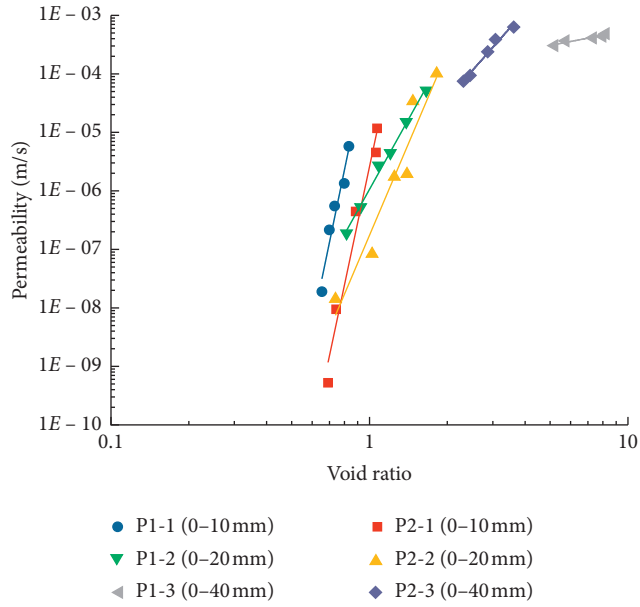

Figure 8: Relationship between the permeability and the void ratio of samples with different particle sizes.

Table 5: Values of coefficients E and F and correlation coefficient R^2.

Sample	P1-1	P1-2	P1-3	P2-1	P2-2	P2-3
E	−3.57	−5.94	−4.11	−5.59	−6.76	−6.76
F	21.45	7.94	0.85	20.86	10.40	5.01
R^2	0.930	0.993	0.906	0.962	0.910	0.973

permeability of the samples with smaller particle sizes decreased to a greater extent at a decreasing void ratio.

The best-fit line of P1-1 was above that of P2-1 in the void ratio range of 0.6–0.9, indicating that the permeability of P1-1 was greater than that of P2-1. The best-fit line of P1-2 was above that of P2-2 in the void ratio range of 0.7–1.6, indicating that the permeability of P1-2 was greater than that of P2-2. The interparticle voids were similar with the same void ratio. The main reason could be that the content of plastic in samples P2-1 and P2-2 was more than that in samples P1-1 and P1-2 for the same void ratio. The vertical seepage path was prolonged because of the large-sized plastics, and the corresponding permeability decreased [17].

3.2.4. Relationship between Permeability and Average Particle Size. Biogas produced from the degradation of organic materials reduces the permeability of MSW [27]. However, the content of organic materials in the MBT waste was relatively low, with less biogas to be produced. The permeability decreased mainly with the decrease in the void ratio. The distributions of the void ratio and permeability were different at different average particle sizes. Figure 9 shows the relationships between the permeability, void ratio, and average particle size.

The figure shows that the permeability increases with the increase in the average particle size and void ratio in the samples P1-1, P1-2, and P1-3 as well as samples P2-1, P2-2, and P2-3. The permeability of P1-1 ranged from 10^{-8} to 10^{-5} m/s with an average particle size of 5.4 mm and a void ratio range of 0.65–0.84. The permeability of P1-2 ranged from 10^{-7} to 10^{-4} m/s with an average particle size of 9.6 mm and a void ratio range of 0.8–1.7. The permeability of P1-3 ranged from 10^{-4} to 10^{-3} m/s with an average particle size of 13.8 mm and a void ratio range of 5.1–8.2. This may be due to the increase in the average particle size, decrease in the content of fines in samples P1-1, P1-2, and P1-3, and decrease in the interparticle voids in samples with smaller particle sizes. The multiple independent seepage channels gradually expanded into a single seepage channel, and the seepage channel widened significantly. The seepage path was significantly reduced, and the permeability increased.

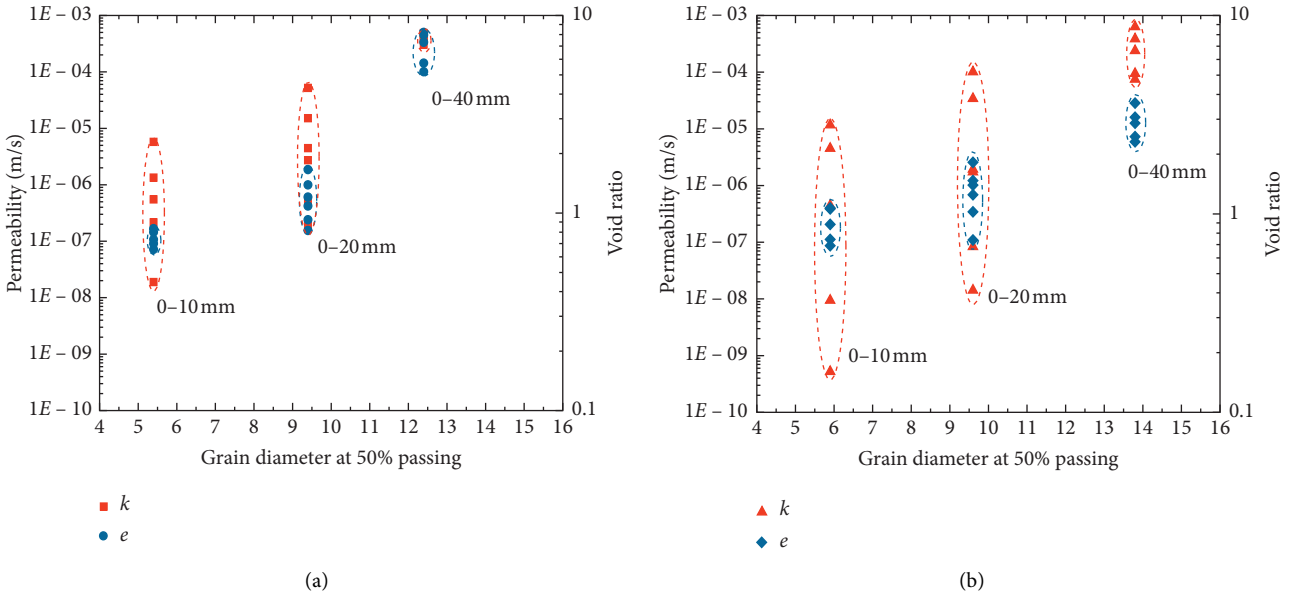

Figure 9: Relationship between permeability, void ratio, and average particle size. (a) P1-1, P1-2, and P1-3. (b) P2-1, P2-2, and P2-3.

The permeability of P2-1 ranged from 10^{-10} to 10^{-5} m/s with an average particle size of 5.9 mm and a void ratio range of 0.66–0.82. The permeability of P2-2 ranged from 10^{-8} to 10^{-4} m/s with an average particle size of 9.4 mm and a void ratio range of 0.7–1.8. The permeability of P2-3 ranged from 10^{-5} to 10^{-3} m/s with an average particle size of 12.4 mm and a void ratio range of 2.3–3.6. The type and dry mass (%) of the components in the samples P2-1, P2-2, and P2-3 were the same, and the increase in the average particle size produced an equivalent effect as the size. The uniformity coefficients of samples P2-1, P2-2, and P2-3 increased with the increase in the average particle size. The larger particle size samples had greater heterogeneity among the components such as plastic and textile. The permeability increased more with larger particle sizes.

4. Discussion

4.1. Comparison of the Results of MBT Waste Samples in China and Some Countries. The difference in the particle size of the waste was found to be significant. The relationship between permeability and the dry density of MSW with different particle sizes was obtained. The permeability of samples with smaller particle sizes was found to be lower. The main reason was that the particle size decreases with degradation [28]. Compared with MSW, the degradable components in the MBT waste were less, and the particle size was mainly related to the MBT process. Figure 10 shows a comparison of the permeability results of the MBT waste. The permeability gradually increases with an increase in the dry density, and the best-fit line between the logarithmic permeability and the dry density is linear. The absolute values of the slope of best-fit line of the samples (Kuehle-Weidemeier [9]; Siddiqui [13]; P1-2) are between those of the samples P1-1 and P1-3. This indicates that the decrease in the permeability of the samples with size ranges of 0–20 and 0–30 mm was greater than that of the samples with a size range of 0–40 mm and less than that of the samples with a size range of 0–10 mm as the dry density increased. The best-fit line (Siddiqui [13]) was located below the best-fit line of P1-2 in the dry density range of 0.45–0.65 g/cm^3, indicating that the permeability (Siddiqui [13]) was low. The main reason could be the different grain size distributions. The average particle size (Siddiqui et al. [29]) was smaller than that of P1-2. The components with a particle size less than 5 mm in the sample (Siddiqui et al. [29]) were more than those in the sample P1-2. The best-fit line (Kuehle-Weidemeier [9]) almost coincided with the best-fit line of P1-2, indicating that the hydraulic characteristics were similar. The main reason was that the average particle size (Kuehle-Weidemeier [9]) was lower than that of P1-2, and the uniformity coefficients were similar. In summary, the degree of uniformity and the distribution of the pores were similar.

4.2. Comparison of the Permeability of MBT Waste and MSW. Figure 11 shows a comparison of the permeability of MBT waste and MSW considering the effects of dry density and average particle size. The distribution range of the MBT waste (Kuehle-Weidemeier [9]; Xie et al. [17]; Siddiqui [13]; this paper) is below that of MSW (Reddy et al. [28]; Jie et al. [30]), indicating that the permeability of MBT waste is less than that of MSW. The particle size of the MBT waste was reduced by mechanical treatment, and the content of the organic materials was reduced through biological treatment. The permeability of the MBT waste and MSW decreased with the increase in the dry density for the same average particle size; the permeability of MBT waste with a lower dry density and that of MSW with a higher dry density were the same. The distribution range of the permeability of MBT

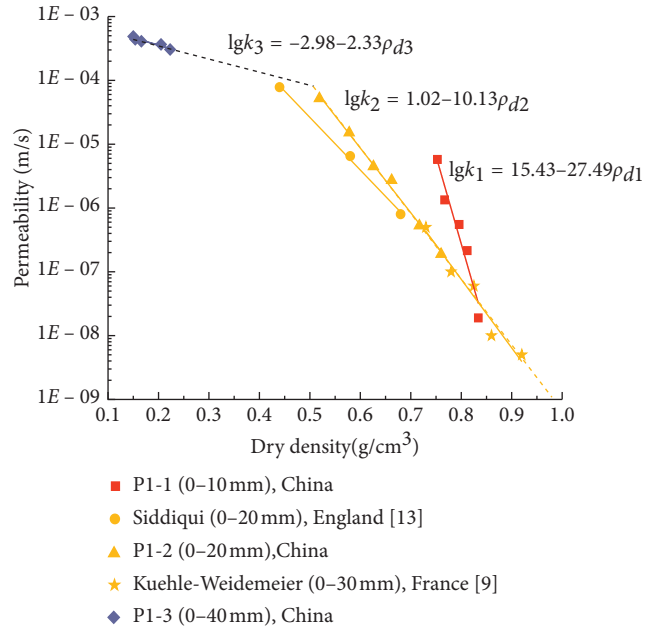

Figure 10: Comparison of permeability of MBT waste in China and some countries.

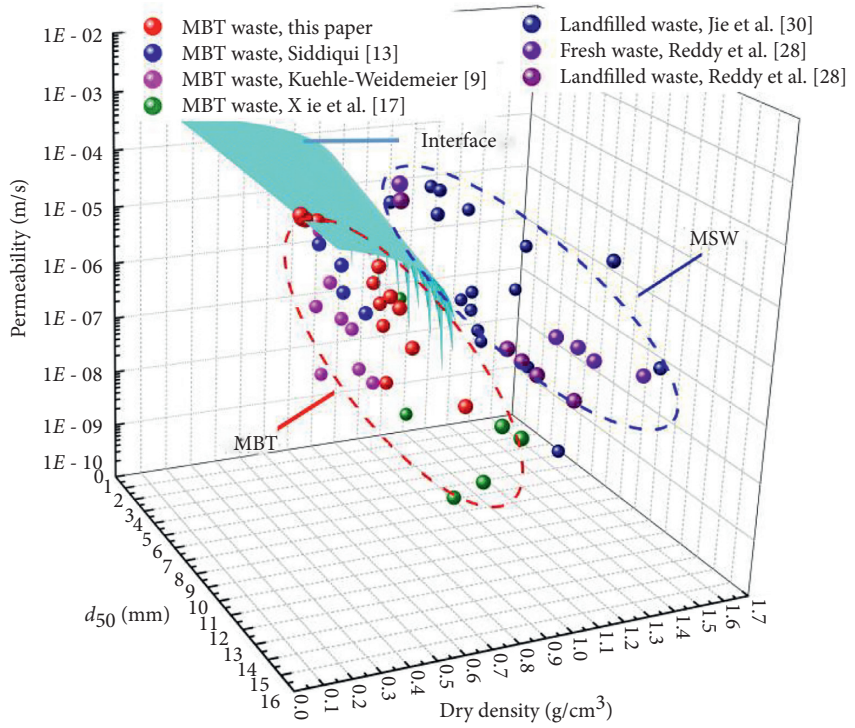

Figure 11: Comparison of permeability of MBT waste and MSW.

waste and MSW generally increased with the increase in the average particle size at the same dry density.

5. Conclusions

Permeability tests were conducted on MBT waste (obtained from the Tianziling Landfill in Hangzhou) with different particle sizes using a compression and permeability combined apparatus and a large-scale vertical permeability apparatus. The following conclusions can be drawn from the study results:

(1) The components in the waste samples were related to the particle sizes. The components of plastics and textiles in the MBT waste were mainly of large size.

Samples of P1-1, P1-2, P1-3, P2-2, P2-3, and the original MBT waste were well-graded waste, whereas P2-1 was not.

(2) The permeabilities of the samples of P1-1, P2-1, P1-2, and P2-2 decreased as the pressure increased, and a pressure of 150 kPa was the critical value. For the same component content and pressure, the permeability of samples with a smaller particle size was lower.

(3) As the particle size increased, the difference in the slopes of the best-fit lines between the logarithmic permeability and the dry density of the samples (P1-1 and P2-1, P1-2 and P2-2, and P1-3 and P2-3) increased. At the same dry density (0.7 g/cm^3), the permeability of P1-1 was 1-2 orders of magnitude greater than those of P1-2 and P1-3. The permeability of samples with smaller particle sizes decreased to a greater extent with the increase in the dry density.

(4) With the increase in the particle size, the absolute values of the slopes of the best-fit lines between the logarithmic permeability and the logarithmic void ratio of samples P1-1, P1-2, and P1-3 decreased sequentially and those of samples P2-1, P2-2, and P2-3 decreased in this order as well. As the void ratio decreased, the permeability of samples with a smaller particle size decreased to a greater extent.

(5) As the average particle size increased, the permeability and void ratio increased. The permeability of samples P1-1, P1-2, and P1-3 ranged from 10^{-8} to 10^{-5}, 10^{-7} to 10^{-4}, and 10^{-4} to 10^{-3} m/s, with average particle sizes of 5.4, 9.6, and 13.8 mm and void ratio ranges of 0.65–0.84, 0.8–1.7, and 5.1–8.2, respectively.

(6) A comparison of the results of MBT waste from China with those from other countries shows that the absolute values of the slopes of the best-fit lines (0–20 and 0–30 mm) were between those of the best-fit lines (0–10 and 0–40 mm) at increasing dry density. A comparison of the permeability of MBT waste with that of MSW shows that the distribution of the permeability of MBT waste was below that of MSW, and the permeability was relatively low.

Data Availability

The data used to support the findings of this study are included within the article.

Conflicts of Interest

The authors declare that they have no conflicts of interest regarding the publication of this paper.

Acknowledgments

This research was funded by the National Natural Science Foundation of China (contract nos. 51678532 and 51978625) and supported by the Fundamental Research Funds of Zhejiang Sci-Tech University (Contract no. 2019Y002). Thanks are due to the Hangzhou Environmental Group for their help.

References

[1] K. Leikam, "Mechanical-biological pretreatment of residual municipal solid waste and the landfill behaviour of pretreated waste," in *Proceedings of the Sixth International Landfill Symposium*, pp. 463–473, Sardinia, Italy, October 1997.

[2] W. Müller, K. Fricke, and H. Vogtmann, "Biodegradation of organic matter during mechanical biological treatment of MSW," *Compost Science & Utilization*, vol. 6, no. 3, pp. 42–52, 1998.

[3] K. Münnich, G. Ziehmann, and K. Fricke, "Biological pretreatment of municipal solid waste in low income countries," in *Proceedings of the International Symposium on Environmental Pollution Control and Waste Management*, pp. 293–303, Tunis, Tunesia, 2002.

[4] E. Trulli, N. Ferronato, V. Torretta, S. Masi, and I. M. Mancini, "Sustainable mechanical biological treatment of solid waste in urbanized areas with low recycling rates," *Waste Management*, vol. 71, pp. 556–564, 2018.

[5] K. Kulhawik, "Direct landfill disposal versus mechanical biological treatment (MBT)," *Ochrona Srodowiska I Zasobów Naturalnych*, vol. 27, no. 3, pp. 19–23, 2016.

[6] J. F. Wagner, G. Rettenberger, and P. Reinert, "Modern landfill technology-landfill behavior of mechanical-biological pre-treated waste," in *Proceedings of the 11th International Waste Management and Landfill Symposium*, pp. 50–60, Sardinia, Italy, 2007.

[7] F. Adani, F. Tambone, and A. Gotti, "Biostabilization of municipal solid waste," *Waste Management*, vol. 24, no. 8, pp. 775–783, 2004.

[8] Y. Zhang, S. Kuschbrandt, S. Gu, and S. Heaven, "Particle size distribution in municipal solid waste pre-treated for bioprocessing," *Resources*, vol. 8, no. 4, 2019.

[9] M. Kuehle-Weidemeier, "Landfilling of mechanically-biologically pre-treated municipal solid waste," in *Proceedings of the International Symposium Waste Management*, Zagreb, Croatia, 2004.

[10] D. Tungtakanpoung, "Characteristics of solid waste after mechanical biological treatment (MBT): a case study of Phitsanulok, Thailand," *Journal of Research in Engineering and Technology*, vol. 3, no. 3, pp. 241–251, 2006.

[11] F. Lombardi, D. L. M. Chiara, A. Lieto, and P. Sirini, "Investigating the leaching properties of MBT wastes and composts from aerobic/anaerobic processes," *Ambiente E Agua-An Interdisciplinary Journal of Applied Science*, vol. 13, no. 1, pp. 1–14, 2018.

[12] G. Ziehmann, K. Münnich, and K. Fricke, "Deposition of mechanical-biologically treated municipal solid waste," in *Proceedings of the 9th International Waste Management and Landfill Symposium*, pp. 768–778, Cagliari, Italy, October 2003.

[13] A. A. Siddiqui, "Pretreated municipal solid waste behaviour in laboratory scale landfill," *International Journal of Sustainable Development and Planning*, vol. 9, no. 2, pp. 263–276, 2014.

[14] G. Ziehmann, K. Münnich, and K. Fricke, "Reduction of leachate volume by mechanical-biological treatment of solid waste," in *Proceedings of International Symposium and Workshop on Environmental Pollution Control and Waste Management*, pp. 454–472, Tunis, Tunesia, January 2002.

[15] C. Heiss-Ziegler and K. Fehrer, "Geotechnical behaviour of mechanically-biologically pretreated municipal solid waste (MSW)," in *Proceedings of the Ninth International Waste Management and Landfill Symposium*, Sardinia, Italy, 2003.

[16] C. Felske, E. Kraft, V. Ustohalova, R. Widmann, and W. Bidlingmaier, "Experimental analysis of the large scale behavior of MBP waste—new results for the design future landfills," in *Proceedings of 9th International Waste Management and Landfill Symposium*, pp. 6–10, Cagliari, Italy, October 2003.

[17] M. Xie, D. Aldenkortt, J.-F. Wagner, and G. Rettenberger, "Effect of plastic fragments on hydraulic characteristics of pretreated municipal solid waste," *Canadian Geotechnical Journal*, vol. 43, no. 12, pp. 1333–1343, 2006.

[18] I. Petrović, V. Szavits-Nossan, and D. Kovačić, "Deformability of municipal waste after biomechanical treatment," *Građevinar*, vol. 63, no. 3, pp. 255–264, 2011.

[19] N. D. Woodman, A. A. Siddiqui, W. Powrie, A. Stringfellow, R. P. Beaven, and D. J. Richards, "Quantifying the effect of settlement and gas on solute flow and transport through treated municipal solid waste," *Journal of Contaminant Hydrology*, vol. 153, pp. 106–121, 2013.

[20] R. L. d. S. Izzo, C. F. Mahler, and J. L. Rose, "Barreira capilar construída com resíduo pré-tratado mecânica e biologicamente," *Engenharia Sanitaria e Ambiental*, vol. 18, no. 4, pp. 303–312, 2013.

[21] P. Pimolthai and J. F. Wagner, "Soil mechanical properties of MBT waste from Luxembourg, Germany and Thailand," *Songklanakarin Journal of Science & Technology*, vol. 36, no. 6, pp. 701–709, 2014.

[22] K. Zardava, W. Powrie, and J. White, "Laboratory experiments for measuring the moisture retention characteristics of MBT waste," in *Proceedings of the 4th International Workshop "Hydro-Physico-Mechanics of Landfills,"* pp. 27-28, Santander, Spain, April 2011.

[23] Z. Zhang, Y. Zhang, W. Guo, D. Wu, and Y. Wang, "Laboratory study on the geotechnical properties of MBT waste," *Chinese Journal of Rock Mechanics and Engineering*, vol. 37, no. 9, pp. 2170–2179, 2018.

[24] Z. Y. Zhang, L. F. Zhang, L. J. Yan, and D. Z. Wu, "Authorized patent: a compression and permeability combined apparatus," State Intellectual Property Office (No. 201410350911.7) in Chinese, 2014.

[25] Z. Y. Zhang, L. F. Zhang, Z. K. Ding, D. Z. Wu, and Y. F. Wang, "Authorized Patent: a large-scale vertical permeability apparatus," State Intellectual Property Office (No. 201520717366.0) in Chinese, 2016.

[26] China Architecture and Building Press, *Technical Specification for Soil Test of Landfilled Municipal Solid Waste CJJ/T204–2013*, China Architecture and Building Press, Beijing, China, 2013, in Chinese.

[27] W. Powrie, R. P. Beaven, and A. P. Hudson, "Factors affecting the hydraulic conductivity of waste," in *Proceedings of the International Workshop, Hydro-Physico-Mechanics of Landfills*, Grenoble, France, March 2005.

[28] K. R. Reddy, H. Hettiarachchi, N. Parakalla, J. Gangathulasi, J. Bogner, and T. Lagier, "Hydraulic conductivity of MSW in landfills," *Journal of Environmental Engineering*, vol. 135, no. 8, pp. 677–683, 2009.

[29] A. A. Siddiqui, W. Powrie, and D. J. Richards, "Impact of pretreatment on the landfill behaviour of MBT waste," in *WIT Transactions on Ecology and the Environment, Sustainable Development and Planning*, vol. 173, pp. 627–638, WIT Press, Southampton, UK, 2013.

[30] Y.-X. Jie, W.-J. Xu, D. Dunzhu, Y.-F. Wei, T. Peng, and Z.-Y. Zhou, "Laboratory testing of a densified municipal solid waste in Beijing," *Journal of Central South University*, vol. 20, no. 7, pp. 1953–1963, 2013.